

Forum Original Research Communication

Mercury-Induced Apoptosis in Human Lymphocytes: Caspase Activation Is Linked to Redox Status

BRUCE J. SHENKER,¹ LISA PANKOSKI,¹ ALI ZEKAVAT,¹ and IRVING M. SHAPIRO²

ABSTRACT

There is growing evidence that heavy metals, in general, and mercurial compounds, in particular, are toxic to the human immune system. We have previously shown that methyl mercuric chloride (MeHgCl) is a potent human T-cell apoptogen; moreover, mitochondria appear to be a target organelle for the induction of cell death. The objective of this study was to determine the impact of MeHgCl on mitochondrial function in lymphocytes in terms of modulating reactive oxygen species (ROS) generation, thiol status, and caspase activation. Using the fluorescent probe, 3,3'-dihexyloxacarbocyanine, we demonstrated that exposure to MeHgCl for 1 h resulted in a profound decrease in the mitochondrial transmembrane potential. We next observed the release of cytochrome *c* from mitochondria into the cytosol; significant translocation was noted between 4 and 8 h following treatment with mercury. ROS generation was monitored by following the conversion of dihydroethidium to the fluorescent product, ethidium. Kinetic analysis indicated that ROS generation was maximal after 16 h of exposure to MeHgCl. The toxicant also depleted the thiol reserves of the cell; glutathione levels were depleted in a dose-dependent fashion reaching minimal levels at 16 h. Real-time RT-PCR analysis demonstrated a significant reduction in both glutathione *S*-transferase and glutathione peroxidase gene expression in mercury-treated cells. Finally, after 16 h of treatment with MeHgCl, we observed activation of caspase-8, -9, and -3 along with increased expression of caspase-8 and -9. We propose that the target organelle for MeHgCl is the mitochondrion and that induction of oxidative stress is critical to activation of death- signaling pathways. Additionally, mercury acts as a genotoxin significantly altering the expression of genes that affect cell survival and apoptosis. *Antioxid. Redox Signal.* 4, 379–389.

INTRODUCTION

THE TOXIC EFFECTS OF MERCURY are directly related to chemical species, dose, target tissue, and route of exposure. Several studies have documented that acute exposure to high levels of methylmercury leads to neurotoxicity, whereas occupational exposure to mercury chloride adversely affects renal function (3, 4, 7, 23). More recently, there has been an increasing concern that chronic low-level exposure to mercury may compromise the immune system.

The mechanism by which mercury acts as an immunotoxin is not well understood and clinical sequelae to expo-

sure are often paradoxical. For example, there is evidence that exposure to both organic and inorganic mercury results in immune activation leading to allergy and autoimmune disease (8, 13, 32, 56, 57, 60). In contrast, both mercury species have also been shown to be cytotoxic. In this case, low-level exposure can trigger lymphocytic immunodeficiency and result in chronic and/or recurrent infection (19, 26, 40, 41, 47). Although these observations may be contradictory, it is more likely that they reflect differences in mercury speciation, as well as animal susceptibility. It is important to note that the few studies that have been conducted on human cells consistently demonstrate impaired

Departments of ¹Pathology and ²Biochemistry, University of Pennsylvania School of Dental Medicine, Philadelphia, PA.

lymphocyte, monocyte, and neutrophil function (11, 12, 26, 36, 39, 47, 55).

Over the past several years, we have focused our investigations on the immunotoxic effects of mercurials on human lymphoid cells. To date, our studies have clearly demonstrated that mercuric compounds represent a potent class of immunotoxins that reduce lymphoid cell (T and B lymphocytes, as well as monocytes) function. Using a wide range of techniques that assess physical, biochemical, and/or molecular properties, we have clearly shown that mercury-treated cells die in a manner consistent with the induction of apoptosis (22, 50). Prior to death, mercury-treated cells exhibit a profound decrease in the adenine nucleotide energy charge ratio, an elevation in $[Ca^{2+}]_i$, and alterations in membrane function; these include altered phospholipid synthesis, loss of normal lipid packing, and the translocation of phosphatidylserine from the inner to the outer surface of the plasma membrane (46, 50). Mercury-treated cells also display morphologic alterations often associated with apoptosis, such as a decrease in cell size and a progressive increase in nuclear condensation with eventual loss of organelle structure.

Although the apoptotic process is regulated at a number of different levels, mitochondria can play a pivotal role in directing the cascade of events that ultimately lead to cell death. In this regard, we have shown that low-level mercury exposure causes functional and morphologic alterations in mitochondria consistent with the activation of the apoptotic cascade. Morphologically, the mitochondria of mercury-treated cells exhibit a decrease in length and diameter, as well as loss of the regular organization of the cristae (51, 52). Moreover, as a result of the development of the membrane permeability transition, mitochondrial function is compromised. Thus, the mitochondria of mercury-treated cells exhibit a profound reduction in the transmembrane potential ($\Delta\Psi_m$). When this occurs, there is mitochondrial uncoupling and the electron flow is also disturbed. In addition, reactive oxygen species (ROS) are generated; these two events conspire to activate cell death. Changes in mitochondrial membrane function result in opening of the mitochondrial megapores and release of cytochrome *c*. The association of cytochrome *c* with a second released protein (Apaf-1) and dATP serves to form an apoptosome that recruits, binds, and activates procaspase-9. Once activated, this enzyme activates procaspase-3, an executioner enzyme that triggers destruction of cell proteins. These activities occur concomitantly with ROS generation and loss of thiol reserve. How mercury affects each of these events in lymphocytes has not been elucidated. The major objective of this investigation was to examine the impact of methyl mercuric chloride (MeHgCl) on mitochondrial function in lymphocytes in terms of temporal relations with ROS, thiol status, and activation of caspase-8, -9, and -3.

MATERIALS AND METHODS

Cell isolation and culture

Blood was obtained from healthy donors whose blood mercury burden was below detectable levels; donors were 22–40 years of age and included both genders. Also, replicate

experiments used different donors, and no individual variation in the effective dose response to mercury was noted. Human peripheral blood mononuclear cells (HPBMC) were isolated by buoyant density centrifugation on Ficoll–Hypaque as previously described (50). For selected experiments, purified populations of T-cells were obtained from the HPBMC by the E-rosette technique (49). Following rosetting, cells were centrifuged on Ficoll–Hypaque and the rosetted T-cells in the pellet were lysed to remove the sheep erythrocytes. When stained with anti-CD3 monoclonal antibody (Becton–Dickinson Immunocytometry Systems, San Jose, CA, U.S.A.) and analyzed by flow cytometry, this fraction contained >98% T-cells. Lymphocyte cultures (1 ml) containing 2×10^6 cells were established in 24-well tissue culture plates in medium containing RPMI 1640 (GIBCO, Grand Island, NY, U.S.A.) and 2% human AB serum. Cell cultures were treated with varying amounts of MeHgCl (ICN Pharmaceuticals, Irvine, CA, U.S.A.) for 1–16 h; the cells were then washed and used for studies described below.

Flow cytometric analysis of mitochondria transmembrane potential ($\Delta\Psi_m$), ROS generation, and caspase activation

Perturbations in $\Delta\Psi_m$ were monitored by flow cytometry using a modification of the method described by Castedo *et al.* (6). In brief, T-cells were exposed to mercury for varying periods of time as indicated above. $\Delta\Psi_m$ was measured directly using 40 nM 3,3'-dihexyloxacarbocyanine [$DiOC_6(3)$] (Molecular Probes, Eugene, OR, U.S.A.). Fluorescence was measured after the cells were stained for 15 min at 37°C. The probe was excited with a laser at 488 nm (250 mW); $DiOC_6(3)$ emission was measured through a 530/30 nm bandpass filter. To assess ROS generation by flow cytometry, cells were treated with 2 μM dihydroethidium for 15 min at 37°C; fluorescence was excited with a laser at 488 nm (250 mW) and emission detected with a 575/26 nm bandpass filter. Logarithmic amplification was used to detect the fluorescence of both probes.

Caspase activation was monitored using the following carboxyfluorescein (FAM)-labeled fluoromethyl ketone (FMK) peptide inhibitors of caspase-8, -9, and -3: FAM-LETD-FMK (caspase-8), FAM-LEHD-FMK (caspase-9), and FAM-DEVD-FMK (caspase-3) (Intergen Co., Purchase, NY, U.S.A.). These inhibitors irreversibly bind to the active caspase. Fluorescein isothiocyanate fluorescence was detected as previously described (53).

Measurement of intracellular glutathione (GSH) levels and glutathione S-transferase activity

T-cells were prepared for GSH measurement as described by Gmunder *et al.* (17). Cells were harvested and washed in phosphate-buffered saline; cell pellets were resuspended in ice-cold 2.5% sulfosalicylic acid (Sigma Chemical Co., St. Louis, MO, U.S.A.) and sonicated. The cells were then centrifuged and the supernatant aliquoted. GSH assays were performed using a modification of previously described methods (1, 48, 58). In brief, equal volumes of cell extract were mixed with assay buffer containing 1 mM 5,5'-dithio-bis(2-nitrobenzoic acid) (Sigma Chemical Co.), 1 mM NADPH, 1 mM EDTA, and 5

units of glutathione reductase in phosphate buffer, pH 7.5. The rate of thionitrobenzoate formation was monitored at 412 nm for 7 min.

Relative levels of GSH were also determined in T-cells by using the reporter molecule, monochlorobimane (MCB), in conjunction with flow cytometric analysis (43). Cell cultures were prepared as described above and stained for 10 min with MCB (10 μ g/ml); MCB fluorescence was excited with a laser operated at 310 nm (80 mW) and emission detected through a 450/50 nm band pass filter.

To measure glutathione *S*-transferase activity, T-cells were homogenized and centrifuged at 1,000 *g* and the supernatant collected. The cell supernatant (400 μ l) was mixed with 1 mM 1-chloro-2,4-dinitrobenzene (Sigma Chemical Co.) and 2.5 mM GSH (Sigma Chemical Co). After 6 min, the absorbance at 340 nm was determined. The enzyme activity was calculated: 1 μ mol of 1-chloro-2,4-dinitrobenzene utilized per minute ($\Delta\epsilon_{340} = 9.6$ mM).

Analysis of cytochrome *c* translocation

Mercury-treated T-cells were suspended in extraction buffer containing 220 mM mannitol, 68 mM sucrose, 50 mM PIPES-KOH, pH 7.4, 50 mM KCl, 5 mM EGTA, 2 mM $MgCl_2$, 1 mM dithiothreitol, 10 μ M cytochalasin B, 1 mM phenylmethylsulfonyl fluoride, and 10 μ g/ml each of leupeptin, chymostatin, antipain, and pepstatin. After 30 min on ice, cells were disrupted with a glass homogenizer as described by Kluck *et al.* (25) and centrifuged at 14,000 *g* for 15 min, 30 μ g of cytosolic protein was then fractionated by sodium dodecyl sulfate–polyacrylamide gel electrophoresis and analyzed by western blot analysis with anti-cytochrome *c* monoclonal antibody (PharMingen, San Diego, CA, U.S.A.). The blots were developed with goat anti-mouse Ig conjugated to horseradish peroxidase (Southern Biotech; Birmingham, AL, U.S.A.) utilizing chemiluminescence (DuPont NEN, Boston, MA, U.S.A.).

Real time RT-PCR analysis of mRNA

Replicate cultures of lymphocytes were pooled (50 \times 10⁶ cells), and RNA was extracted from lysed cells with 5 ml of Trisol (Gibco Life Technologies) according to the manufacturer's instructions and then resuspended in 50 μ l of diethyl pyrocarbonate-treated water. RNA quantification was performed by spectrophotometry; the RNA preparation was considered acceptable for further use if the A_{260}/A_{280} ratio was between 1.8 and 2.1. Reverse transcription was performed on aliquots of RNA (5 μ g) using the SuperScript First-Strand Synthesis System (Gibco Life Technologies) according to the

manufacturer's directions, and the reaction products were stored at $-20^{\circ}C$.

The real-time RT-PCR assay used the double-stranded DNA-specific dye SYBR Green I (FastStart DNA Master SYBR Green I kit; Roche Diagnostics) and PCR performed on a LightCycler [(Roche Diagnostics) (44)]. cDNA amplification was carried out in 20- μ l samples containing 2 μ l of reverse-transcribed cDNA (1:5 dilution), 0.2 μ M primer (see Table 1), 4 mM $MgCl_2$, SYBR Green I, deoxynucleoside triphosphate mix, and FastStart Taq DNA polymerase. After an initial denaturation at 95 $^{\circ}C$ for 10 min, the reactions were cycled through the LightCycler (45 cycles): denaturation of 1 s at 95 $^{\circ}C$, annealing for 5 s at 55 $^{\circ}C$ (glutathione peroxidase) or at 58 $^{\circ}C$ (glutathione *S*-transferase), and elongation of 15 s at 72 $^{\circ}C$. The primers and product are described in Table 1; identity and specificity of the PCR product were confirmed by melting curve analysis and electrophoresis. The relative amount of PCR product in each sample was calculated using the LightCycler software; in brief, crossing points (threshold cycles) were determined based on the log- linear portion of the amplification curve (31).

RESULTS

The objective of this study was to establish the temporal relationship between the decline in $\Delta\Psi_m$, the generation of ROS, the change in thiol status, and the activation of caspases in mercury-exposed lymphocytes. T-cells were treated with MeHgCl for varying periods of time and then stained with both DiOC₆(3) and dihydroethidium to measure the $\Delta\Psi_m$ and generation of superoxide anion (O₂^{•-}), respectively (Fig. 1). Multiparameter FACS analysis indicated that the majority of control cells (75%) are characterized as exhibiting bright DiOC₆(3) fluorescence and virtually no ethidium fluorescence (Fig. 1A; lower right quadrant). Thus, these cells generate minimum levels of ROS and possess mitochondria with high $\Delta\Psi_m$. After exposure to MeHgCl for 2 h, 87% of the cells exhibited a decrease in the DiOC₆(3) fluorescence, which is consistent with a decline in the $\Delta\Psi_m$ (Fig. 1B; lower left quadrant). At this time point, only 4% of these cells were generating ROS (ethidium fluorescence; upper left quadrant). Similar results were observed following 4 and 6 h of treatment with MeHgCl (Fig. 1C and D). Significant ROS generation was not observed until the cells had been exposed to MeHgCl for 16 h; at this time point, 95% of the cells exhibited low DiOC₆(3) fluorescence and 51% were also positive for ethidium fluorescence (Fig. 1E; upper left quadrant). To learn if the loss of membrane potential triggered cytochrome *c* release

TABLE 1. PRIMERS USED TO AMPLIFY TARGET GENE FRAGMENTS

Gene	Forward primer	Reverse primer	PCR product (nucleotides)
Glutathione <i>S</i> -transferase	CTATGATGTCCTTGACCTCCACCGTATA	ATGTTACACGAAGGATAGTGGGTAGCTGA	402
Glutathione peroxidase	CCCTCTGAGGCACACGGT	TAAGCGCGGTGGCGTCGT	291

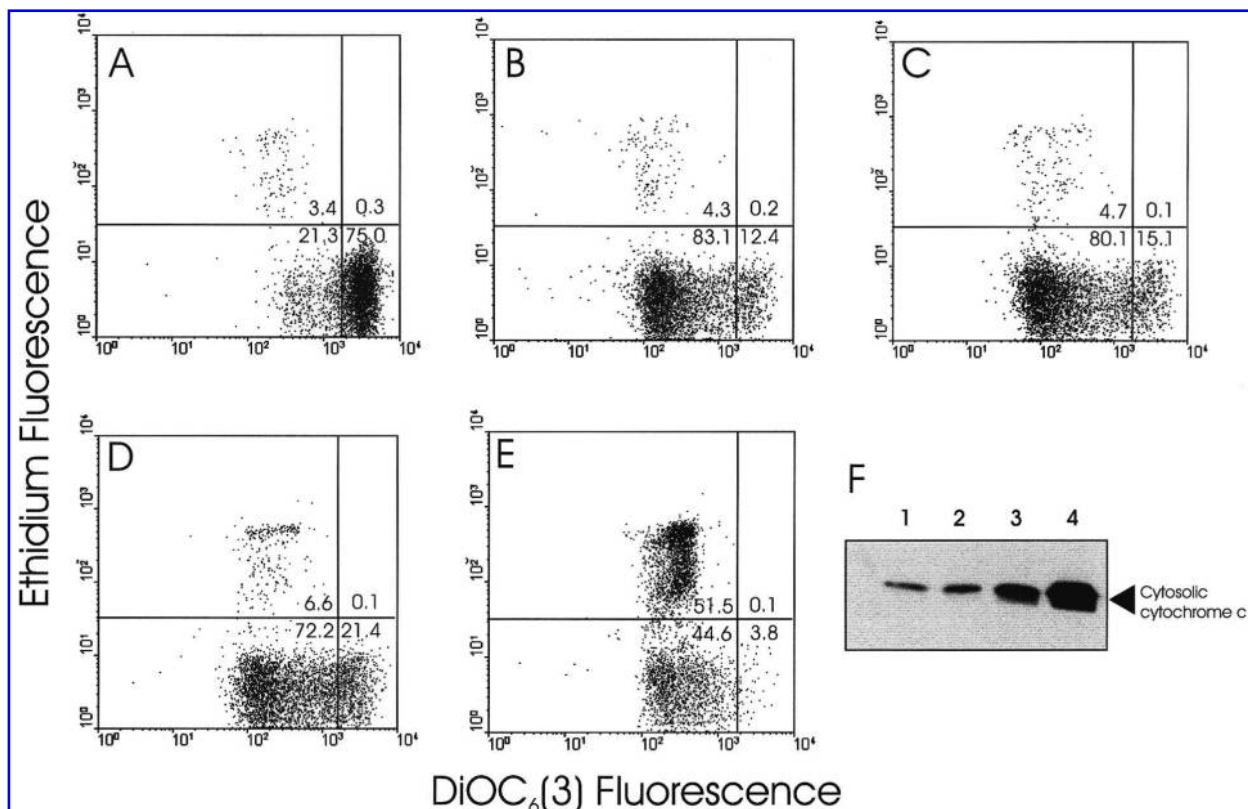


FIG. 1. Temporal relationship between the decline in $\Delta\Psi_m$, the generation of $O_2^{\bullet-}$, and the release of cytochrome *c* into the cytosol. T-cells were incubated in the absence (A) or presence of 1.5 μM MeHgCl for 2 h (B), 4 h (C), 6 h (D) or 16 h (E). The cells were stained with DiOC₆(3) and dihydroethidium simultaneously to monitor the $\Delta\Psi_m$ and generation of $O_2^{\bullet-}$. Numbers represent the percentage of cells in each quadrant. Results are representative of five experiments; at least 10,000 cells were analyzed per sample. **F:** Western blot analysis of cytosolic cytochrome *c*. T-cells were incubated in the presence of medium alone (lane 1) or 1.5 μM MeHgCl (LD_{50}) for 2 h (lane 2), 4 h (lane 3), or 8 h (lane 4). The cells were then disrupted, and the cytosol fraction was collected, fractionated by sodium dodecyl sulfate–polyacrylamide gel electrophoresis, and analyzed for cytochrome *c* content by western blot. The relative amounts of cytochrome *c* were determined by scanning densitometry; values were 642 (control), 901 (2 h), 2,745 (4 h), and 5,673 (8 h). Note: a 40% increase in cytosolic cytochrome *c* was observed within 2 h of exposure to MeHgCl; the cytosolic concentration of cytochrome *c* reached maximum levels of almost ninefold above control at 8 h.

from mitochondria, western blot analysis was performed. Western blot analysis indicated that at short time periods (0–2 h), there was a minimal level of release of cytochrome *c* into the cytosol. In contrast, 4 h following exposure to MeHgCl, there was a threefold increase in cytosolic cytochrome *c*, and by 8 h these levels increased eightfold (Fig. 1F).

As ROS generation can serve to lower the cells' reductive reserve, we also determined the effect of MeHgCl on T-cell GSH content (Fig. 2A). The resting level of GSH in untreated T-cells was 1.1 nmol/10⁶ cells. Following exposure to MeHgCl for 16 h, a dose-dependent reduction in the GSH concentration was observed. We also determined the level of oxidized glutathione disulfide (GSSG) in the treated cells. We noted that the concentration of this thiol level was not affected by the presence of mercury; however, the resting level of GSSG in T-cells was very low, and hence it was difficult to detect any alteration due to mercury (data not shown). Not only was the GSH content reduced, the activity of glutathione *S*-transferase was also diminished in MeHgCl-treated cells

(Fig. 2A); thus, mercury-treated cells have a diminished capacity to reduce $O_2^{\bullet-}$ and other ROS. The effect of MeHgCl on GSH levels over time was also monitored by measuring MCB fluorescence levels. As shown in Fig. 3A, control cells exhibited the highest GSH content with a mean channel MCB fluorescence of 287. Exposure of lymphocytes to MeHgCl for 2 h (Fig. 3B) resulted in a slight decline in GSH content; mean channel MCB fluorescence was 230. Similar results were observed at 4 h (data not shown). A significant reduction in GSH levels was observed after 6 h of exposure to MeHgCl [mean channel MCB fluorescence was 168 (Fig. 3C)]. The GSH content was further reduced after 16 h of exposure; mean channel MCB fluorescence was reduced to 74.

Previous studies have suggested that mercury may also influence gene expression (11). Therefore, we also analyzed mercury-treated cells for levels of glutathione *S*-transferase and glutathione peroxidase mRNA by real-time RT-PCR. Amplification plots are presented in Fig. 2B and C. Comparisons for each curve were performed based upon the threshold

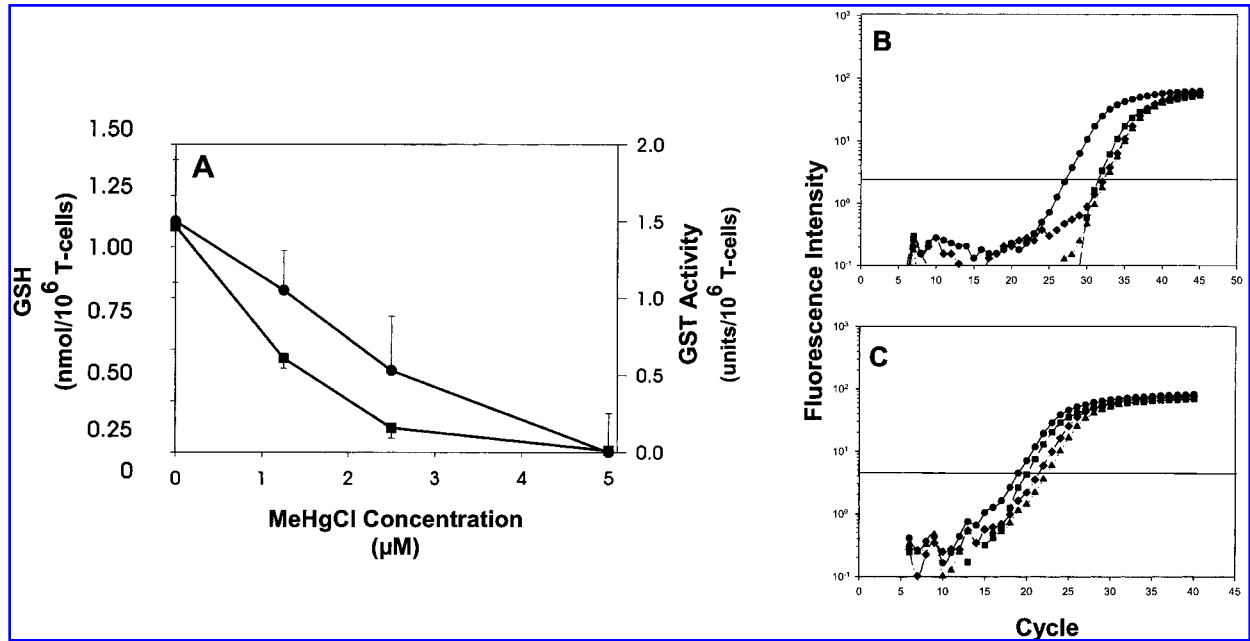


FIG. 2. Effect of MeHgCl on cellular GSH levels, glutathione *S*-transferase (GST) activity, and gene expression. (A) Effect of MeHgCl on GSH content and GST activity. T-cells were incubated with 0–5 μM MeHgCl for 16 h. Cells were prepared as described in Materials and Methods and analyzed for GSH content (circles) and GST activity (squares). Results are plotted as GSH content (nmol/ 10^6 cells) or GST activity (units/ 10^6 cells) versus MeHgCl concentration. Note: MeHgCl treatment results in a dose-dependent reduction in GSH content and GST activity. The results represent the means \pm SEM of three experiments. (B and C) Amplification plots of real-time RT-PCR for GST (B) and glutathione peroxidase (C). The plots were prepared by plotting cycle versus fluorescence intensity for control cells (circles) or cells treated with 1.5 μM MeHgCl for 2 h (triangles), 4 h (squares), or 8 h (diamonds). The horizontal line represents the threshold cycle (C_T).

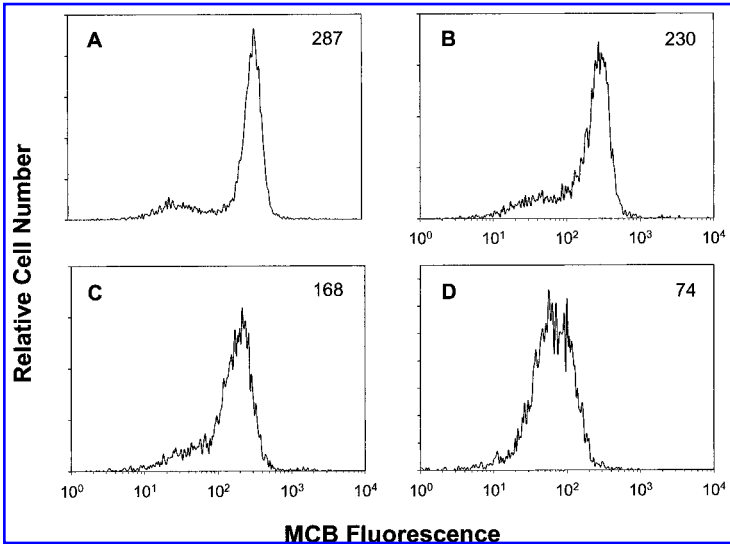


FIG. 3. Temporal relationship of the effect of MeHgCl on GSH content. T-cells were incubated in medium (A) or in the presence of 2.5 μM MeHgCl for 2 h (B), 6 h (C) or 16 h (D); the cells were then stained with MCB and analyzed by flow cytometry. Numbers represent the mean MCB fluorescence. Results are representative of three experiments; at least 20,000 cells were analyzed.

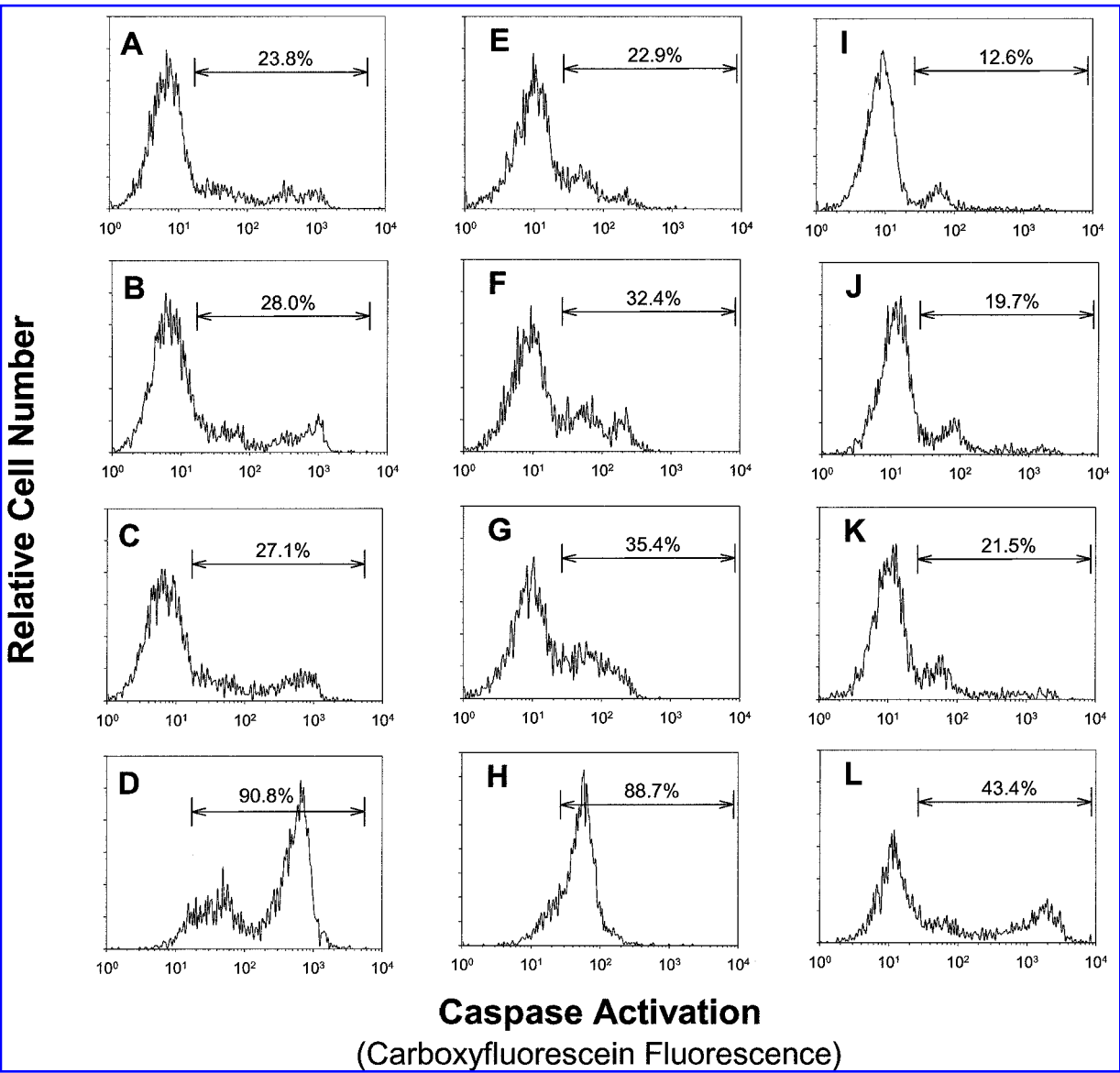


FIG. 4. Effect of MeHgCl on caspase activation. HPBMC were pretreated with medium alone (A, E, and I) or 1.5 μ M MeHgCl for 3 h (B, F, and J), 6 h (C, G, and K) or 16 h (D, H, and L). The cells were then assessed for caspase activation using the fluorescent caspase inhibitors: FAM-LETD-FMK (caspase-8; A–D), FAM-LEHD-FMK (caspase-9; E–H), and FAM- DEVD-FMK (caspase-3; I–L). Stained cells were analyzed by flow cytometry. Bars indicate region of positive fluorescence; the percentage of positive cells is presented in each panel. Results are representative of two experiments.

cycle (C γ); the larger the starting copy number, the lower the C γ . The highest level of expression of both glutathione S-transferase and glutathione peroxidase was found in the control cultures with C γ values of 28.7 and 19.9, respectively. Within 2 h following exposure to MeHgCl, there was a significant decline in the transcript levels of both genes. The C γ was 33.5 for glutathione S-transferase and 23.1 for glutathione peroxidase; this represents a decrease to <10% of the transcript levels observed in the control cultures. Transcript levels remained depressed for both genes following 8 h of exposure to MeHgCl, although we did observe a rebound at 4 h.

Perturbation of mitochondrial function and the translocation of cytochrome *c* to the cytosol have been shown to be important prerequisites for the activation of the caspase cascade. To monitor caspase activation, we utilized specific fluorescent caspase inhibitors of caspase-8 (FAM-LETD-FMK), caspase-9 (FAM-LEHD-FMK), and caspase-3 (FAM-DEVD-FMK), which irreversibly bind to active caspases. As shown in Fig. 4A, E, and I, the percentage of control cells that exhibited caspase-8, -9, and -3 activation was 23%, 22%, and 12%, respectively. There was a slight increase in caspase activation in cells treated with MeHgCl for 3 and 6 h: 28% and 27%

(caspase-8), 32% and 35% (caspase-9), and 19% and 21% (caspase-3), respectively (Fig. 4B, C, F, G, J, and K). In contrast, there was a significant increase in the percentage of cells exhibiting caspase-8 (90%), caspase-9 (88%), and caspase-3 (43%) activation 16 h following exposure to MeHgCl (Fig. 4D, H, and L).

DISCUSSION

The goal of this investigation was to explore the relationship between mercury exposure, mitochondrial function, thiol status, and caspase activation. Results of the investigation clearly suggest a pivotal role for mitochondria in mercury-induced T-cell death and further define a sequence of events that lead to activation of the apoptotic cascade. First, we noted a rapid decline in the $\Delta\Psi_m$ within 1 h of exposure to MeHgCl. We next observed the release of cytochrome *c* from mitochondria into the cytosol; significant translocation was noted between 4 and 8 h following treatment with mercury. Finally, after 16 h of treatment with MeHgCl, we observed an increase in the generation of ROS; this event was accompanied by a profound depletion in thiols and activation of caspase-8, -9, and -3. From the sequence of events, we infer that MeHgCl impairs normal mitochondrial function causing a subsequent liberation of ROS and loss of thiol reserve, thereby modulating the cytosolic environment that enhances caspase activation and ultimately the induction of the apoptotic cascade.

The earliest sign of mitochondrial involvement is the development of a membrane permeability transition and a decrease in the $\Delta\Psi_m$. We probed the $\Delta\Psi_m$ of MeHgCl-treated cells using the fluorescent dye DiOC₆(3); uptake of this dye into the mitochondria is almost entirely electrogenic and driven by the $\Delta\Psi_m$. The negatively charged energized inner membrane binds the cationic lipophilic fluorochrome and provides a measure of $\Delta\Psi_m$ (28, 29, 37). Changes in the $\Delta\Psi_m$ leading to the development of the permeability transition result in the opening of the transmembrane megapore channels that are thought to be regulated by the Bcl-2 family of pro- and antiapoptotic proteins (10, 27, 63). Once open, a number of mitochondrial associated proteins are released into the cytoplasm; these proteins include cytochrome *c*, Apaf-1, and apoptosis-inducing factor (9, 18, 25, 33, 38, 42, 54, 64). Cytochrome *c* and Apaf-1 oligomerize to form the apoptosome, a complex that recruits and binds caspase-9. The apoptosome is then able to activate, by autocatalytic cleavage, this enzyme, which in turn cleaves and activates the executioner caspases 3, 6, and 7 (5, 20, 64). Indeed, we have shown that caspase-3 and -6 are activated in lymphocytes 16 h following exposure to low levels of MeHgCl. Thus, perturbation of mitochondrial function leading to the release of cytochrome *c* and the formation of the apoptosome is critical not only to apoptosis in general, but also to the apoptogenic effects of mercury, in particular.

We also observed that mercury activates caspase-8. This caspase is normally associated with upstream events linked to receptor-mediated apoptosis (2, 21). Relevant to these observations, several investigators have reported that caspase-8

may be activated via receptor-independent mechanisms (16). Furthermore, in their studies of drug-induced apoptosis, Essman *et al.* (14) recently suggested that caspase-8 activation occurred downstream of caspase-3. Thus, it is possible that once activated, caspase-3 and other executioner caspases cleave and activate the upstream caspases. This event could serve to amplify the cascade and facilitate the death process.

In addition to the loss of $\Delta\Psi_m$ and cytochrome *c* release, we have previously shown that mercury-treated cells also exhibit alterations in pH_i, ATP depletion, and a low adenylate energy charge (39, 51, 52). Thus, the mitochondria are unable to maintain the electrogenic and protonmotive forces required to generate the $\Delta\Psi_m$ and preserve mitochondrial function. ATP depletion would in itself damage the cell due to failure to provide energy for membrane pumps; a greater hazard, however, is the generation of ROS. Although a number of systems exist in lymphocytes to synthesize free radicals, the most important ROS generator is the electron transport chain. When the function or integrity of the chain is compromised, for example, by treatment with uncoupling agents, mitochondria generate excessive amounts of oxygen radicals. Accumulation of radicals has been shown to be an effective mechanism to activate the apoptotic cascade (15, 30, 34, 45, 62, 65). There are several mechanisms by which ROS may induce apoptosis. First, it is likely that binding of mercury to membranes, and the loss of coupling, generates ROS. These short-lived, short-range species are then free to enhance lipid and protein peroxidation chain reactions in the mitochondrial membrane, thereby exacerbating organelle dysfunction. We have in fact previously reported that the mitochondrial membrane phospholipid, cardiolipin, undergoes oxidation in the presence of mercury (52). Second, ROS may activate caspases directly. Indeed, caspases are activated in a reducing environment (59), and caspase-3, in particular, is regulated by redox status of the cell (61). A third possibility is that low levels of ROS may be rapidly generated and dismutated in cells shortly after exposure to MeHgCl. In this case, O₂^{•-} would serve in a signaling capacity to trigger the caspase cascade. Our results clearly indicate that the ROS generation is indeed a consequence of exposure to mercury; this is a relatively late event occurring at about the same time that the caspases are activated. It should be noted, however, that the methods used in this study lack the sensitivity to detect low levels of ROS.

Loss of mitochondrial function is further aggravated when there is a decline in thiol reserves, because molecules such as GSH scavenge ROS and protect membranes from oxidative damage. We have shown that the decrease in GSH levels proceeds in parallel with the generation of ROS. Thus, it is tempting to speculate that ROS cause the decline in reductive reserve. In addition, a loss of thiol groups may be due to mercury ions oxidizing thiols to form mixed additive compounds (-S-Hg; -S-Hg-S-).

Results of the study provide evidence that MeHgCl inhibits glutathione *S*-transferase activity and that there is a profound decrease in its expression. Furthermore, real-time RT-PCR indicated that glutathione peroxidase expression is profoundly impaired by mercury. Accordingly, mercury interferes with the thiol reserve of the cell by preventing both its regeneration and its utilization. These observations are consistent with results of our previous studies, as well as those of

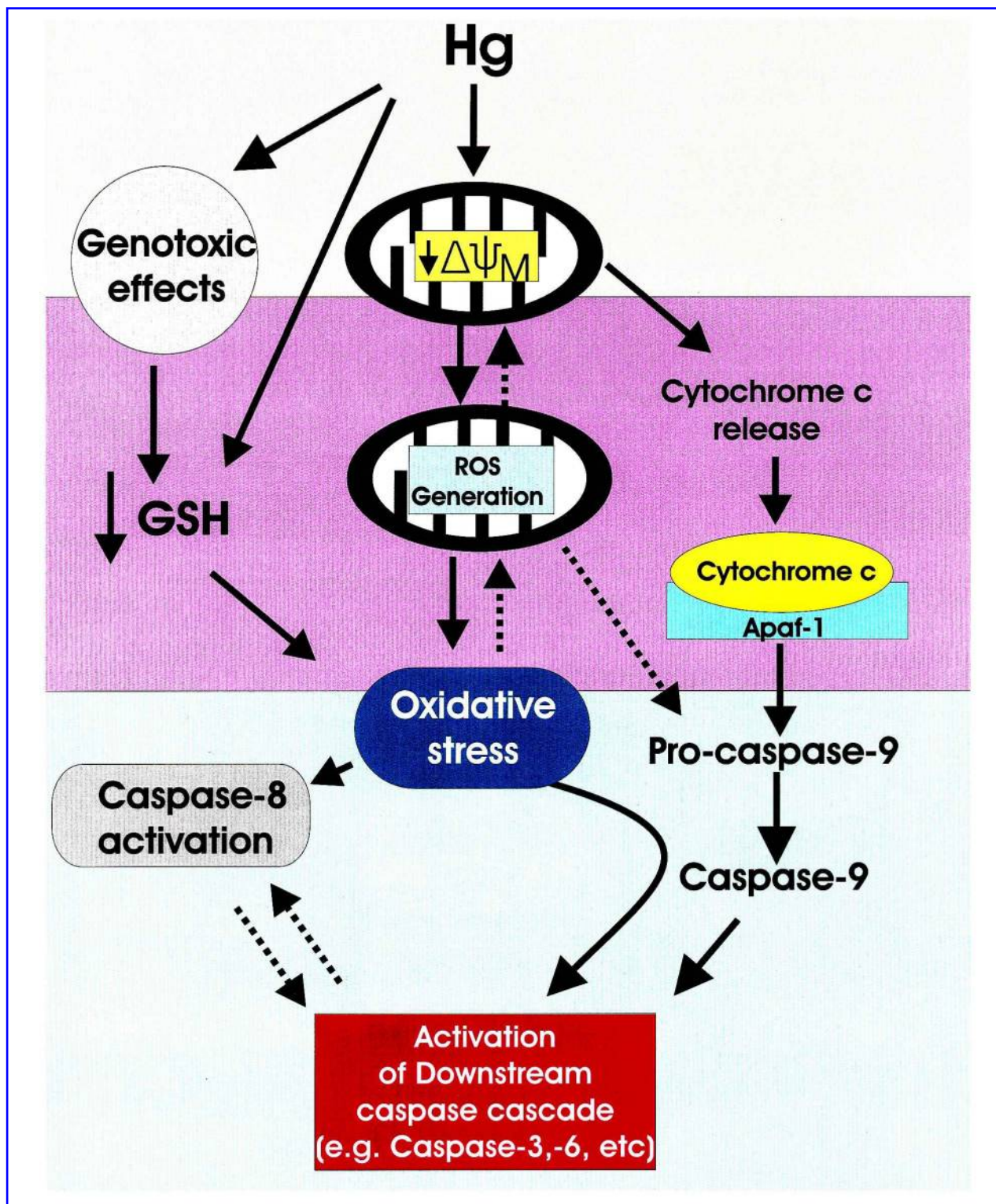


FIG. 5. Schematic representation of MeHgCl-induced apoptosis. Mercury-induced apoptosis can be envisioned as occurring in three phases: an early inductive phase (yellow background), a later effector phase (pink background), and a late degradative phase (blue background). Collectively, our studies indicate that mitochondria are pivotal to the induction of apoptosis by MeHgCl. MeHgCl first induces a profound decline in the $\Delta\Psi_m$, which ultimately leads to the translocation of cytochrome *c* to the cytoplasm, formation of the apoptosome, and caspase activation. However, caspase activation does not occur for 16 h when a state of oxidative stress develops. Oxidative stress is the combined result of ROS generation by the perturbed mitochondria and a decline in thiol reserve, which is due, in part, to genotoxic events that impair the expression of genes critical to the recycling and utilization of GSH.

other workers, where a linkage between mercury toxicity and depletion of cellular thiols was demonstrated (24, 35, 48, 65). It is likely that the low GSH levels predispose the cell to ROS damage, thereby attenuating death signaling pathways.

In summary, based on our experimental findings (summarized in Fig. 5), we propose that the primary effects of mercury are twofold: degradation of mitochondrial function and depletion of thiol reserves. The induction of oxidative stress, which is specifically associated with the induction of the mitochondrial permeability transition and the loss of reductive reserve, leads to the formation of the apoptosome and activation of the caspase cascade. However, it should also be noted that mercury is genotoxic because profound changes are apparent in the expression of genes that influence cell survival and apoptosis. Knowledge of the apoptotic pathway itself may provide therapeutic approaches and the design of drugs that serve to counteract the insidious effect of this highly toxic element.

ACKNOWLEDGMENTS

The authors wish to acknowledge the technical expertise of Terry McKay and Dave Besack and the support of the SDM Flow Cytometry Facility. This work was supported by USPHS grant DE 10873.

ABBREVIATIONS

DiOC₆(3), 3,3'-dihexyloxacarbocyanine; FAM, carboxyfluorescein; FMK, fluoromethyl ketone; GSH, glutathione; GSSG, oxidized glutathione disulfide; HPBMC, human peripheral blood mononuclear cells; MCB, monochlorobimane; MeHgCl, methyl mercuric chloride; O₂⁻, superoxide anion; ROS, reactive oxygen species; $\Delta\Psi_m$, transmembrane potential.

REFERENCES

- Anderson ME. Determination of glutathione disulfide in biological samples. *Methods Enzymol* 113: 548–555, 1985.
- Ashkenazi A and Dixit VM. Apoptosis control by death and decoy receptors. *Curr Opin Cell Biol* 11: 255–260, 1999.
- Ashour H, Abdel-Rahman M, and Khodair A. The mechanism of methyl mercury toxicity in isolated rat hepatocytes. *Toxicol Lett* 69: 87–96, 1993.
- Atchison WD and Hare MF. Mechanisms of methylmercury-induced neurotoxicity. *FASEB J* 8: 622–629, 1994.
- Bossy-Wetzel E and Green DR. Apoptosis: checkpoint at the mitochondrial frontier. *Mutat Res* 434: 243–251, 1999.
- Castedo M, Macho A, Zamzami N, Hirsch T, Marchetti P, Uriel J, and Kroemer G. Mitochondrial perturbations define lymphocytes undergoing apoptotic depletion *in vivo*. *Eur J Immunol* 25: 3277–3284, 1995.
- Clarkson TW. The toxicology of mercury. *Crit Rev Clin Lab Sci* 34: 369–403, 1997.
- Dantas DCM and Queiroz MLS. Immunoglobulin E and autoantibodies in mercury-exposed workers. *Immunopharmacol Immunotoxicol* 19: 383–392, 1997.
- Daugas E, Nochy D, Ravagnan L, Loeffler M, Susin SA, Zamzami N, and Kroemer G. Apoptosis inducing factor (AIF): a ubiquitous mitochondrial oxidoreductase involved in apoptosis. *FEBS Lett* 476: 118–123, 2000.
- Decaudin D, Geley S, Hirsch T, Castedo M, Marchetti P, Macho A, Kofler R, and Kroemer G. Bcl-2 and Bcl-XL antagonize the mitochondrial dysfunction preceding nuclear apoptosis induced by chemotherapeutic agents. *Cancer Res* 57: 62–67, 1997.
- De Flora S, Bennicelli C, and Bagnasco M. Genotoxicity of mercury compounds. A review. *Mutat Res* 317: 57–79, 1994.
- Descotes J, Nicholas B, and Vial T. Assessment of immunotoxic effects in humans. *Clin Chem* 41: 1870–1873, 1995.
- Dieter MP, Luster MI, Boorman GA, Jameson CW, Dean JH, and Cox JW. Immunological and biochemical responses in mice treated with mercuric chloride. *Toxicol Appl Pharmacol* 68: 218–228, 1983.
- Essman W, Prokop A, Schmelz K, Schulze-Osthoff K, Beyaert R, Dorken B, and Daniel PT. Activation of caspase-8 in drug-induced apoptosis of B-lymphoid cells is independent of CD96/Fas receptor-ligand interaction and occurs downstream of caspase-3. *Blood* 97: 1378–1387, 2001.
- Gansauge S, Gansauge F, Gause H, Poch B, Schoenberg MH, and Beger HG. The induction of apoptosis in proliferating human fibroblasts by oxygen radicals is associated with a p53- and p21^{WAF1/CIP1} induction. *FEBS Lett* 404: 6–10, 1997.
- Gao C, Ren S, Nakajima T, Ichinose S, Hara T, Koike K, and Tsuchida N. Caspase-dependent cytosolic release of cytochrome *c* and membrane translocation of bax in p53-induced apoptosis. *Exp Cell Res* 265: 145–151, 2001.
- Gmunder H, Eck HP, Benninghoff B, Roth S, and Droge W. Macrophages regulate intracellular glutathione levels of lymphocytes. Evidence for an immunoregulatory role of cysteine. *Cell Immunol* 129: 32–46, 1990.
- Golstein P. Controlling cell death. *Science* 275: 1081–1082, 1997.
- Gopinath C. Pathology of toxic effects on the immune system. *Inflamm Res* 45: S74–S78, 1996.
- Green DR. Apoptotic pathways: the roads to ruin. *Cell* 94: 695–698, 1998.
- Grutter MG. Caspases: key players in programmed cell death. *Curr Opin Struct Biol* 10: 643–655, 2000.
- Guo TL, Miller M, Shapiro IM, and Shenker BJ. Mercuric chloride induces apoptosis in human T lymphocytes: evidence of mitochondrial dysfunction. *Toxicol Appl Pharmacol* 153: 250–257, 1998.
- Harada M. Minamata disease: methylmercury poisoning in Japan caused by environmental pollution. *Crit Rev Toxicol* 25: 1–24, 1995.
- Iwata S, Hori T, Sato N, Hirota K, Sasada T, Mitsui A, Hirakawa T, and Yodoi J. Adult T cell leukemia (ATL)-derived factor/human thioredoxin prevents apoptosis of lymphoid cells induced by L-cysteine and glutathione depletion. *J Immunol* 158: 3108–3117, 1997.

25. Kluck RM, Bossy-Wetzel E, Green DR, and Newmeyer DD. The release of cytochrome *c* from mitochondria: a primary site for Bcl-2 regulation of apoptosis. *Science* 275: 1132–1136, 1997.
26. Koropatnick J and Zalups RK. Effect of non-toxic mercury, zinc or cadmium pretreatment on the capacity of human monocytes to undergo lipopolysaccharide-induced activation. *Br J Pharmacol* 120: 797–806, 1997.
27. Kroemer G. The proto-oncogene Bcl-2 and its role in regulating apoptosis. *Nat Med* 3: 614–620, 1997.
28. Kroemer G, Petit P, Zamzami N, Vayssiere J, and Mignotte B. The biochemistry of programmed cell death. *FASEB J* 9: 1277–1287, 1995.
29. Kroemer G, Zamzami N, and Susin SA. Mitochondrial control of apoptosis. *Immunol Today* 18: 44–51, 1997.
30. Langer C, Jurgensmeier JM, and Bauer G. Reactive oxygen species act at both TGF- β -dependent and -independent steps during induction of apoptosis of transformed cells by normal cells. *Exp Cell Res* 222: 117–124, 1996.
31. Lara-Marquez ML, O'Dorisio MS, O'Dorisio TM, Shah MH, and Karacay B. Selective gene expression and activation-dependent regulation of vasoactive intestinal peptide receptor type 1 and type 2 in human T cells. *J Immunol* 166: 2522–2530, 2001.
32. Lawrence D. Heavy metal modulation of lymphocyte activation. I. In vitro effects of heavy metals on primary humoral immune responses. *Toxicol Appl Pharmacol* 57: 439–451, 1981.
33. Li P, Nijhawan D, Budhihardjo I, Srinivasula SM, Ahmad M, Alnemri ES, and Wang X. Cytochrome *c* and dATP-dependent formation of Apaf-1/caspase-9 complex initiates an apoptotic protease cascade. *Cell* 91: 479–489, 1997.
34. Lin K-T, Xue J-Y, Sun FF, and Wong PY-K. Reactive oxygen species participate in peroxynitrite-induced apoptosis in HL-60 cells. *Biochem Biophys Res Commun* 230: 115–119, 1997.
35. Macho A, Hirsch T, Marzo I, Marchetti P, Dallaporta B, Susin SA, Zamzami N, and Kroemer G. Glutathione depletion is an early and calcium elevation is a late event of thymocyte apoptosis. *J Immunol* 158: 4612–4619, 1997.
36. Malamud D, Dietrich S, and Shapiro IM. Low levels of mercury inhibit the respiratory burst in human polymorphonuclear leukocytes. *Biochem Biophys Res Commun* 128: 1145–1151, 1985.
37. Marchetti P, Hirsch T, Zamzami N, Castedo M, Decaudin D, Susin SA, Masse B, and Kroemer G. Mitochondrial permeability transition triggers lymphocyte apoptosis. *J Immunol* 157: 4830–4836, 1996.
38. Medina V, Edmonds B, Young GP, James R, Appleton S, and Zalewski PD. Induction of caspase-3 protease activity and apoptosis by butyrate and trichostatin A (inhibitors of histone deacetylase): dependence on protein synthesis and synergy with a mitochondrial/cytochrome *c*-dependent pathway. *Cancer Res* 57: 3697–3707, 1997.
39. O I, Datar S, Koch CJ, Shapiro IM, and Shenker BJ. Mercuric compounds inhibit human monocyte function by inducing apoptosis: evidence for formation of reactive oxygen species, development of mitochondrial membrane permeability transition and loss of reductive reserve. *Toxicology* 124: 211–224, 1997.
40. Osorio E, Toledano M, Bravo M, and Osorio R. Short-term changes in lymphocytes after placement of silver amalgam restorations in healthy subjects. *Dent Mater* 11: 323–326, 1995.
41. Pollard KM and Hultman P. Effects of mercury on the immune system. *Met Ions Biol Sys* 34: 421–440, 1997.
42. Reed JC. Cytochrome *c*: can't live with it—can't live without it. *Cell* 91: 559–562, 1997.
43. Rice GC, Bump EA, Shrieve DC, Lee W, and Kovacs M. Quantitative analysis of cellular glutathione by flow cytometry utilizing monochlorobimane: some applications to radiation and drug resistance *in vitro* and *in vivo*. *Cancer Res* 46: 6105–6110, 1986.
44. Rokbi B, Seguin D, Guy B, Mazarin V, Vidor E, Mion F, Cadoz M, and Quentin-Millet M. Assessment of *Helicobacter pylori* gene expression within mouse and human gastric mucosae by real-time reverse transcriptase PCR. *Infect Immun* 69: 4759–4766, 2001.
45. Satoh T, Enokido Y, Aoshima H, Uchiyama Y, and Hatanaka H. Changes in mitochondrial membrane potential during oxidative stress-induced apoptosis in PC12 cells. *J Neurosci Res* 50: 413–420, 1997.
46. Shenker BJ, Berthold P, Decker S, Mayro JS, Rooney C, Vitale LA, and Shapiro IM. Immunotoxic effects of mercuric compounds on human lymphocytes and monocytes. II. Alterations in cell viability. *Immunopharmacol Immunotoxicol* 14: 555–577, 1992.
47. Shenker BJ, Rooney C, Vitale LA, and Shapiro IM. Immunotoxic effects of mercuric compounds on human lymphocytes and monocytes. I. Suppression of T-cell activation. *Immunopharmacol Immunotoxicol* 14: 539–553, 1992.
48. Shenker BJ, Mayro JS, Rooney C, Vitale LA, and Shapiro IM. Immunotoxic effects of mercuric compounds on human lymphocytes and monocytes. IV. Alterations in cellular glutathione content. *Immunopharmacol Immunotoxicol* 15: 273–290, 1993.
49. Shenker BJ, Vitale L, and King C. Induction of human T cells that coexpress CD4 and CD8 by an immunomodulatory protein produced by *Actinobacillus actinomycetemcomitans*. *Cell Immunol* 164: 36–46, 1995.
50. Shenker BJ, Datar S, Mansfield K, and Shapiro IM. Induction of apoptosis in human T-cells by organomercuric compounds: a flow cytometric analysis. *Toxicol Appl Pharmacol* 143: 397–406, 1997.
51. Shenker BJ, Guo TL, and Shapiro IM. Low-level methylmercury exposure causes human T-cells to undergo apoptosis: evidence of mitochondrial dysfunction. *Environ Res* 77: 149–159, 1998.
52. Shenker BJ, Guo TL, O I, and Shapiro IM. Induction of apoptosis in human T-cells by methyl mercury: temporal relationship between mitochondrial dysfunction and loss of reductive reserve. *Toxicol Appl Pharmacol* 157: 23–35, 1999.
53. Shenker BJ, Hoffmaster RH, Zekavat A, Yamaguchi N, Lally ET, and Demuth DR. Induction of apoptosis in human T cells by *Actinobacillus actinomycetemcomitans* cytolethal distending toxin is a consequence of G₂ arrest of the cell cycle. *J Immunol* 167: 435–441, 2001.
54. Srinivasula SM, Ahmad M, Fernandes-Alnemri T, and Alnemri ES. Autoactivation of procaspase-9 by Apaf-1-mediated oligomerization. *Mol Cell* 1: 949–957, 1998.

55. Steffensen IL, Mesna OJ, Andruchow E, Namork E, Hyl-land K, and Andersen RA. Cytotoxicity and accumulation of Hg, Ag, Cd, Cu, Pb and Zn in human peripheral T and B lymphocytes and monocytes *in vitro*. *Gen Pharmacol* 25: 1621–1633, 1994.
56. Stejskal VDM, Cederbrant K, Lindvall A, and Forsbeck M. Melisa-an *in vitro* tool for the study of metal allergy. *Toxicol In Vitro* 8: 991–1000, 1994.
57. Stejskal VDM, Forsbeck M, Cederbrant K, and Asteman O. Mercury-specific lymphocytes: an indication of mercury allergy in man. *J Clin Immunol* 16: 31–40, 1996.
58. Tietze F. Enzymatic method for quantitative determination of nanogram amounts of total and oxidized glutathione: application to mammalian blood and other tissues. *Anal Biochem* 27: 502–522, 1969.
59. Ueda S, Nakamura H, Masutani H, Sasada T, Yonehara S, Takabayashi A, Yamaoka Y and Yodoi J. Redox regulation of caspase-3 (-like) protease activity: regulatory roles of thioredoxin and cytochrome *c*. *J Immunol* 161: 6689–6695, 1998.
60. Warfvinge G and Larsson Å. Contact stomatitis to mercury associated with spontaneous mononuclear cell infiltrates in brown Norway (BN) rats with HgCl₂-induced autoimmunity. *J Oral Pathol Med* 23: 441–445, 1994.
61. Wilson KP, Black J, Thomson J, Kim E, Griffith J, Navia M, Murcko M, Chambers S, Aldape R, Raybuck S, and Livingston DJ. Structure and mechanism of interleukin-1 β converting enzyme. *Nature* 370: 270–274, 1994.
62. Wood KA and Youle RJ. The role of free radicals and p53 in neuron apoptosis *in vivo*. *J Neurosci* 15: 5851–5857, 1995.
63. Yang J, Liu X, Bhalla K, Kim CN, Ibrado AM, Cai J, Peng TI, Jones DP, and Wang X. Prevention of apoptosis by Bcl-2: release of cytochrome *c* from mitochondria blocked. *Science* 275: 1129–1132, 1997.
64. Zou H, Henzel WJ, Liu X, Lutschg A, and Wang X. Apaf-1, a human protein homologous to *C. elegans* CED-4, participates in cytochrome *c*-dependent activation of caspase-3. *Cell* 90: 405–413, 1997.
65. Zucker B, Hanusch J, and Bauer G. Glutathione depletion in fibroblasts is the basis for apoptosis-induction by endogenous reactive oxygen species. *Cell Death Differ* 4: 388–395, 1997.

Address reprint requests to:

Dr. Bruce J. Shenker

Department of Pathology

University of Pennsylvania School of Dental Medicine

4010 Locust Street

Philadelphia, PA 19104-6002

E-mail: shenker@pobox.upenn.edu

Received for publication August 10, 2001; accepted October 29, 2001.

This article has been cited by:

1. Chun-Fa Huang, Shing-Hwa Liu, Shoei-Yn Lin-Shiau. 2012. Pyrrolidine dithiocarbamate augments Hg²⁺-mediated induction of macrophage cell death via oxidative stress-induced apoptosis and necrosis signaling pathways. *Toxicology Letters* **214**:1, 33-45. [[CrossRef](#)]
2. Yangho Kim, Byung-Kook Lee. 2012. Association between blood lead and mercury levels and periodontitis in the Korean general population: analysis of the 2008–2009 Korean National Health and Nutrition Examination Survey data. *International Archives of Occupational and Environmental Health* . [[CrossRef](#)]
3. Marianne Polunas, Alycia Halladay, Ronald B. Tjalkens, Martin A. Philbert, Herbert Lowndes, Kenneth Reuhl. 2011. Role of oxidative stress and the mitochondrial permeability transition in methylmercury cytotoxicity. *NeuroToxicology* . [[CrossRef](#)]
4. Matthew Garrecht, David W. Austin. 2011. The plausibility of a role for mercury in the etiology of autism: a cellular perspective. *Toxicological & Environmental Chemistry* **93**:6, 1251-1273. [[CrossRef](#)]
5. N. Pavon, M. Franco, F. Correa, N. Garcia, E. Martinez-Abundis, D. Cruz, L. Hernandez-Esquivel, J. Santamaria, J. S. Rodriguez, C. Zazueta, E. Chavez. 2011. Octylguanidine ameliorates the damaging effect of mercury on renal functions. *Journal of Biochemistry* **149**:2, 211-217. [[CrossRef](#)]
6. C. T. Mahapatra, J. Bond, D. M. Rand, M. D. Rand. 2010. Identification of Methylmercury Tolerance Gene Candidates in Drosophila. *Toxicological Sciences* **116**:1, 225-238. [[CrossRef](#)]
7. Susana Cuello, Luis Goya, Yolanda Madrid, Susana Campuzano, Maria Pedrero, Laura Bravo, Carmen Cámara, Sonia Ramos. 2010. Molecular mechanisms of methylmercury-induced cell death in human HepG2 cells. *Food and Chemical Toxicology* **48**:5, 1405-1411. [[CrossRef](#)]
8. Denise Grotto, Juliana Valentini, Myriam Fillion, Carlos José Souza Passos, Solange Cristina Garcia, Donna Mergler, Fernando Barbosa Jr.. 2010. Mercury exposure and oxidative stress in communities of the Brazilian Amazon. *Science of The Total Environment* **408**:4, 806-811. [[CrossRef](#)]
9. Dong-Hun Han, Sin-Ye Lim, Bo-Cheng Sun, Sok-Ja Janket, Jin-Bom Kim, Dai-Il Paik, Domyung Paek, Hyun-Duck Kim. 2009. Mercury Exposure and Periodontitis Among a Korean Population: The Shiwha-Banwol Environmental Health Study. *Journal of Periodontology* **80**:12, 1928-1936. [[CrossRef](#)]
10. Rodrigo Franco, Roberto Sánchez-Olea, Elsa M. Reyes-Reyes, Mihalís I. Panayiotidis. 2009. Environmental toxicity, oxidative stress and apoptosis: Ménage à Trois. *Mutation Research/Genetic Toxicology and Environmental Mutagenesis* **674**:1-2, 3-22. [[CrossRef](#)]
11. Tawit Suriyo, Apinya Thiantanawat, Sansanee C. Chaiyaroj, Preeda Parkpian, Jutamaad Satayavivad. 2008. Involvement of the Lymphocytic Muscarinic Acetylcholine Receptor in Methylmercury-Induced c-Fos Expression and Apoptosis in Human Leukemic T Cells. *Journal of Toxicology and Environmental Health, Part A* **71**:16, 1109-1123. [[CrossRef](#)]
12. R. Klaper, B. J. Carter, C. A. Richter, P. E. Drevnick, M. B. Sandheinrich, D. E. Tillitt. 2008. Use of a 15 k gene microarray to determine gene expression changes in response to acute and chronic methylmercury exposure in the fathead minnow *Pimephales promelas* Rafinesque. *Journal of Fish Biology* **72**:9, 2207-2280. [[CrossRef](#)]
13. M PINHEIRO, B MACCHI, J VIEIRA, T OIKAWA, W AMORAS, G GUIMARAES, C COSTA, M CRESPOLOPEZ, A HERCULANO, L SILVEIRA. 2008. Mercury exposure and antioxidant defenses in women: A comparative study in the Amazon. *Environmental Research* **107**:1, 53-59. [[CrossRef](#)]
14. Fusako Usuki, Eriko Fujita, Noboru Sasagawa. 2008. Methylmercury activates ASK1/JNK signaling pathways, leading to apoptosis due to both mitochondria- and endoplasmic reticulum (ER)-generated processes in myogenic cell lines#. *NeuroToxicology* **29**:1, 22-30. [[CrossRef](#)]
15. T COCCINI, G RANDINE, A CASTOLDI, D ACERBI, L MANZO. 2007. Methylmercury interaction with lymphocyte cholinergic muscarinic receptors in developing rats. *Environmental Research* **103**:2, 229-237. [[CrossRef](#)]

16. Kerstin Eisele, Philipp A. Lang, Daniela S. Kempe, Barbara A. Klarl, Olivier Niemöller, Thomas Wieder, Stephan M. Huber, Christophe Duranton, Florian Lang. 2006. Stimulation of erythrocyte phosphatidylserine exposure by mercury ions. *Toxicology and Applied Pharmacology* **210**:1-2, 116-122. [[CrossRef](#)]
17. S ZIEMBA, M MCCABEJR, A ROSENSPIRE. 2005. Inorganic mercury dissociates preassembled Fas/CD95 receptor oligomers in T lymphocytes. *Toxicology and Applied Pharmacology* **206**:3, 334-342. [[CrossRef](#)]
18. A SARMENTO. 2004. Mercury chloride effects on the function and cellular integrity of sea bass (*Dicentrarchus labrax*) head kidney macrophages. *Fish & Shellfish Immunology* **17**:5, 489-498. [[CrossRef](#)]
19. S Kim. 2004. Mercury-induced apoptosis and necrosis in murine macrophages: role of calcium-induced reactive oxygen species and p38 mitogen-activated protein kinase signaling. *Toxicology and Applied Pharmacology* **196**:1, 47-57. [[CrossRef](#)]
20. Sang Hyun Kim, Raghubir P. Sharma. 2003. Cytotoxicity of inorganic mercury in murine T and B lymphoma cell lines: involvement of reactive oxygen species, Ca²⁺ homeostasis, and cytokine gene expression. *Toxicology in Vitro* **17**:4, 385-395. [[CrossRef](#)]
21. Y Suzuki. 2003. Stress-induced activation of GATA-4 in cardiac muscle cells. *Free Radical Biology and Medicine* **34**:12, 1589-1598. [[CrossRef](#)]